10.6 Eddy Formation and Shock Features Associated with a Coastally Trapped Disturbance

William T. Thompson and Stephen D. Burk
Naval Research Laboratory
Monterey, California

1. Introduction

On 28 August 2002, a remarkable sequence of events took place in association with a coastally trapped disturbance (CTD) as it propagated along the coast of northern California[1]. Satellite imagery for the preceding day shows a complete absence of low cloudiness along the coast, symptomatic of strong offshore flow which typically precede CTD events. The CTD (as evidenced by a sharply defined, narrow tongue of stratus) propagates northward against the prevailing northwesterly flow, arriving in Monterey Bay at 11:30 UTC, San Francisco Bay at 14:30 UTC, and reaching Pt. Reyes at 16:30UTC 28 August 2002. As the CTD rounds Pt. Arena, a dramatic, well-defined shock feature develops and angles away from the coast to the southwest. Over the next 3-4 h, the CTD rolls into a striking eddy leeward of Cape Mendocino and another off of Pt. Arena. Similar eddies associated with CTD's have been documented by Dorman (1985) and Rogerson (1999). This sequence of events is well illustrated in an animated satellite loop from 1700 UTC 28 August to 0200 UTC 29 August 2002. Some images from this loop are described and shown in the following. The characteristics and dynamics associated with these phenomena motivated the present study.

During the summer months, a shallow marine boundary layer (MBL) is often present along the southwest coast of North America. The inversion in the upper portion of the MBL typically lies below the top of coastal terrain (Winant et al. 1988; Burk and Thompson 1996). The shallow MBL adjacent to steep coastal terrain can support a variety of mesoscale phenomena. These phenomena include, among other things, CTD's (also referred to as coastally trapped wind reversals) (Bond et al. 1996; Thompson et al. 1997; Ralph et al. 1998;), hydraulic features including expansion fans and compression jumps (Winant et al. 1988; Samelson 1992, Burk et al. 1999) as well as low level jets, land/sea breezes, and mountain-valley winds.

In the present study, we examine the 28 August case. This sequence of events is illustrated using satellite images from the period. Nonhydrostatic mesoscale model simulations of this period using the Naval Research Laboratory COAMPS™[2] model reproduce features of the event seen in satellite images and buoy observations.

2. Modeling Aspects

The COAMPS™ mesoscale model used in the present study is described by Hodur (1997). The model has continued to evolve since the publication date but the basic framework is still consistent with the description given by Hodur. The model is nonhydrostatic and uses multiple nests having different horizontal resolution. It features a full suite of physical parameterizations, including the Mellor and Yamada (1982) level 2.5 turbulence parameterization and sophisticated radiation and cloud microphysics schemes.

In parameterizing boundary layer processes, COAMPS™ uses a prognostic equation for turbulent kinetic energy (TKE) with diagnostic equations for other second moment quantities. The buoyant production of TKE is computed from the virtual buoyancy flux which incorporates the effects of a statistical cloud fraction scheme. The turbulent length scale is a modified Blackadar (1962) scheme which gives a

[1] Corresponding Author Address: Dr. William T. Thompson, Naval Research Laboratory, Marine Meteorology Division, Monterey, CA 93943. thompson@nrlmry.navy.mil

[2] COAMPS is a trademark of the Naval Research Laboratory

more uniform vertical profile under highly unstable conditions. It is constrained to lie between an asymptotic limit determined from the ratio of the first moment to the zeroth moment of the vertical distribution of TKE and a value based on the Brunt-Vaisala length scale used under stable conditions. The eddy coefficients are based on Yamada (1983). Surface fluxes and surface stress are computed from the Louis (1979) scheme. This scheme uses functional fits to Monin-Obukhov similarity theory, yielding flux-profile relationships with Richardson number dependent functions for the exchange coefficients.

The COAMPS™ model simulation of this event utilizes the grid structure shown in Fig 1. As indicated, the horizontal resolution of the nests is 27 km, 9 km, and 3 km. Three 12 h data assimilation forecasts were performed prior to the 12 h forecast beginning at 1200 UTC 28 August depicting the period of interest (a second 12 h forecast beginning at 0000 UTC 29 August is required to span the period of interest).

3. **Case Description**

a. *Synoptic Discussion*

On 27 August 2002, a weak 500 mb trough was located over the western U. S.. At sea level, a ridge over Oregon and Washington resulted in NE offshore flow over Northern California while an inverted thermal trough was located over the southern San Joaquin Valley and the southern deserts of California. On 28 August, the trough at 500 mb deepened significantly. The inverted thermal trough over California deepened as well and extended from just east of Cape Mendocino to South-Central Arizona. The ridge over the Pacific Northwest resulted in continued offshore flow over Northern California.

b. *Mesoscale Evolution*

b. 1 Satellite Imagery

The mesoscale evolution of the event is shown in a series of satellite images from the afternoon of 28 August with buoy and coastal station observations overlaid (Fig 2). The image from 1800 UTC 28 August 2002 (Fig 2a) shows a cloud-free zone along the coast of Southern Oregon and Northern California. There is a large area of low clouds 50-75 km offshore extending along the coast over the domain of the image. The narrow cloud "tongue" south of Pt. Arena is associated with a coastally trapped disturbance (CTD), as indicated by the wind barbs in the buoy observations from Pt. Arena south. Note the strong southerly wind at San Francisco and Monterey. The southerly flow precedes the cloud tongue by several hours, as shown by the buoy at Pt. Arena. This tendency of the with shift to precede the leading edge of the clouds has been noted previously by Ralph et al. (1998) and Thompson et al. (1997). West of Pt. Arena at the edge of the offshore cloud band is a series of wave clouds. There appear to be ~5-6 distinct wave crests reflected in the cloud field. These wave clouds appear to be indicative of trapped gravity waves associated with a compression jump and are similar in appearance to wave clouds discussed by Burk and Haack (2001). Over the next few hours, the tongue of clouds associated with the CTD continues to move north, hugging the immediate coast. The wave clouds become more distinct as they appear to have an albedo significantly larger than the surrounding clouds, despite the fact that all of the clouds visible are within the marine boundary layer. By 2000 UTC, the leading edge of the compression jump/wave clouds is located ~40-50 km north of the position at 1800 UTC. Examination of intermediate satellite images (not shown) confirms that the leading edge of the wave cloud region is propagating to the north rather than remaining stationary as in the case described by Burk and Haack (their case involved supercritical flow interacting with the Monterey Peninsula and had no propagating CTD). The cloud tongue associated with the CTD has also propagated to the north and the cloud edge is north of Pt. Arena. At 2200 UTC (Fig 2b), a rather striking image shows that a pair of cyclonic eddies has formed due to the interaction of the prevailing NW coast-parallel flow and the southerly flow associated with the CTD. The northern eddy is just in the lee of Cape Mendocino and is delineated by fine cloud filaments wrapping around the center. The eddies are both ~50-75 km in diameter. The genesis

and maintenance of the eddies is under investigation. The linear features associated with the compression jump are no longer visible, having apparently been entrained into the northern eddy. The images at 2300 UTC 28 August and at 0000 UTC 29 August show that the eddies continue to be well-defined but are becoming increasingly cloud-filled.

b. 2 Model Forecasts

Shown in Fig 3 are forecasts of 10 m elevation streamlines and integrated cloud liquid water (kg m^{-2}; shaded) over a zoomed area of the inner nest. Figure 3a shows the model 10 h forecast valid 2200 UTC 28 August . At this time, the southerly flow and cloud tongue extend to Pt. Arena and the southern eddy is quite well-defined. The northern eddy is barely discernable and the compression jump is evident as the strong anticyclonic shear zone extending from the northern eddy to the SW. The leading edge of the cloudy region in the NW flow to the west of the coast is visible in the NW corner of the figure. Flow along the entire coast is onshore. Although not evident from the figure, a strong expansion fan (wind speed ~14 m s^{-1}) is located immediately in the lee of Cape Mendocino. The southerly flow is at about 6 ms^{-1}. At 0000 UTC 29 August, the model shock feature has strengthened substantially and propagated to the north in agreement with the satellite images. Both of the model eddies are well-defined and southerly flow extends to just south of Cape Mendocino in a narrow zone along the immediate coast in agreement with the satellite images. The model cloud tongue associated with the CTD has rounded Pt Arena and a clear "slot" is visible over the center of the southern eddy. The cloudy area to the west has advanced toward the coast. Note that the integrated cloud water is much larger within the cloud tongue associated with the CTD than in the cloud shield to the west. At 0200 UTC (Fig 3b), the cloud shield advancing from the west has merged with the cloud tongue and clouds have filled in all along the coast with the exception of the northern eddy, which remains cloud-free (the southern eddy, visible at this time as a cyclonic shear zone, is cloud-filled). The compression jump is no longer apparent.

Also shown in Fig 3 is a cross-section plane extending from 41° N to 38° N in a coast-parallel orientation. Shown in Fig 4 is a cross section of potential temperature (K) and cloud liquid water mixing ratio (g/kg) extending from the surface to 1600 m valid at 2200 UTC 28 August 2002. The extremely shallow marine layer with a strong capping inversion near the center of the cross section is due to the expansion fan in the lee of Cape Mendocino. The extremely sharp perturbation in the isentropes south of the expansion fan is the compression jump. Near the southern end of the cross section, the boundary layer depth is uniform at ~150 m and filled with fog in the CTD advancing to the north.

c. *Comparison with observations*

Propagation of the CTD northward along the coast from Pt. Conception to Pt. Reyes can be tracked from forecasts on nest 2 (not shown). The times at which the wind shift from NW to SE occurs at coastal buoys and in the forecasts at corresponding locations agrees well, indicating that the speed of propagation is well represented.

Comparison of the buoy observations plotted on the satellite image to the model wind field on nest 3 shows general agreement with a time lag of ~2 hours. Two of the buoys lie within the nest 3 domain; these are the Eel River buoy (46022) and the Bodega Bay buoy (46013) (see Fig 1 for locations). Shown in Fig 5 is a time series of wind direction at Bodega Bay from 1200 UTC 28 August to 0000 UTC 29 August. Note that the wind direction at the buoy abruptly shifts to southerly at hour 14 while the model wind direction gradually backs to the south. The model wind direction is due south at 1600 UTC and agrees well with the buoy observation at the following hours. The wind speed (not shown) increases following passage of the CTD to 8 ms^{-1} in the observations and to 7.6 ms^{-1} an hour later in the model. Generally light winds in the model for the first 5 h ($\leq$ 2 ms^{-1}) may be related to the gradual shift to southerly flow.

At Eel River, the model wind direction (Fig 6) and speed are in good agreement with the buoy observation. The direction is consistently from the N through 0600 UTC 29 August (for ease of comparison, wind directions D less than 90° are set equal to

D+360). The wind direction agrees to within ~30^{o} at most hours and the model has a slightly larger easterly component at most hours with the exception of hours 22 and 23. The model wind speed is also stronger than that at the buoy the difference is generally 1 m s^{-1} with the largest difference being just over 2 m s^{-1}.

4. **Discussion and Conclusion**

In the present study, we investigate an event in which a CTD propagating northward along the coast past Point Arena encounters supercritical flow in an expansion fan in the lee of Cape Mendocino. A compression shock forms south of Cape Mendocino, angling away from the coast. The shock feature propagates to the north for several hours and then rolls up into a cyclonic eddy. The Naval Research Laboratory's nonhydrostatic COAMPS model is used to simulate this period. The model results compare quite favorably with satellite imagery and coastal buoy observations. Model forecasts provide a three dimensional context for the surface observations and satellite imagery. Derived quantities such as divergence, vorticity, and Froude Number are computed from model forecast fields in order to investigate the dynamics of the event.

The coastal processes investigated in the present study are not particularly rare; indeed transcritical conditions are found in the lee of points and capes in the mean summer (June-July) climatology (Dorman et al. 2000) and CTD's occur several times each year, often spawning cyclonic eddies in conjunction with cessation of propagation. The event described herein, however, features all of these processes and incorporates the highly nonlinear interaction among them, including the northward propagation of the compression jump, the large variations in boundary layer depth associated with the expansion fan and compression jump which could impede progress of the CTD, and the strong horizontal shear associated with the NW flow offshore and the southerly flow in the CTD which may spawn the cyclonic eddies.

Acknowledgments. We gratefully acknowledge Dr. Peter Guest for bringing this interesting meteorological event to our attention. This research was supported by the Office of Naval Research Program Element 0601153N.

REFERENCES

Bond, N. A., C. F. Mass, and J. E. Overland, 1996: Coastally trapped wind reversals along the United States West Coast during the warm season. Part 1: Climatology and temporal evolution. *Mon. Wea. Rev*., **124**, 430-445.

Blackadar, A. K., 1962: The vertical distribution of wind and turbulent exchange in a neutral atmosphere. *J. Geophys. Res*., **67**, 3095-3103.

Burk, S. D. and T. Haack, 2001: The dynamics of wave clouds upwind of coastal orography. *Mon. Wea. Rev*., **128**, 1438-1455.

Burk, S. D., T. Haack, and R. M. Samelson, 1999: Mesoscale simulation of supercritical, subcritical, and transcritical flows along coastal topography. *J. Atmos. Sci*., **56**, 2780-2795.

Burk, S. D. and W. T. Thompson, 1996: The summertime low-level jet and marine boundary layer structure along the California Coast. *Mon. Wea. Rev*., **124**, 668-686.

Dorman, C. E., 1985 : Evidence of Kelvin waves in Cailfornia's marine layer and related energy generation. *Mon. Wea. Rev*., **113**, 827-839

Dorman, C., T. Holt, D. Rogers, and K. Edwards, 2000: Large-scale structure of the June-July 1996 Marine boundary layer along California and Oregon. *Mon. Wea. Rev*., **128**, 1632-1652.

Hodur, R. M., 1997 : The U. S. Navy's coupled ocean/atmosphere mesoscale prediction system (COAMPS). *Mon. Wea. Rev*., **125**, 1414-1430.

Louis, J.-F., 1979 : A parametric model of vertical eddy fluxes in the atmosphere. *Bound. Layer. Meteor*., **17**, 187-202

Mellor, G. L. and T. Yamada, 1982: Development of a turbulence closure for geophysical problems. *Rev. Geophys. Space Phys*., **20**, 851-875.

Ralph, F. M., L Armi, J. M. Bane, C. Dorman, W. D. Neff, P. J. Neiman, W. Nuss, and P.O.G. Persson , 1998 : Observations and analysis of the 10-11 June coastally trapped disturbance. *Mon. Wea. Rev*., **126**, 2435-2465.

Rogerson, A. M., 1999: Transcritical flows in the coastal marine atmospheric boundary layer. *J. Atmos. Sci*., **56**, 2761-2779.

Samelson, R. M., 1992: Supercritical marine layer flow along a smoothly varying coastline. *J. Atmos. Sci*., **49,** 1571-1584**.**

Thompson, W. T., T. Haack, J. D. Doyle, and S. D. Burk, 1997: A nonhydrostatic mesoscale simulation of the 10-11 June 1994 coastally trapped wind reversal. *Mon. Wea. Rev*., **125**, 3211-3230,

Winant, C. D., C. E. Dorman, C. A. Friehe, and R. C. Beardsley, 1988: The marine layer off northern California: An example of supercritical channel flow. *J. Atmos. Sci*., **45**, 3588-3605.

Yamada, T., 1983 : Simulation of nocturnal drainage flows by a q^{2}l turbulence closure model. *J. Atmos. Sci*., **40**, 91-106,

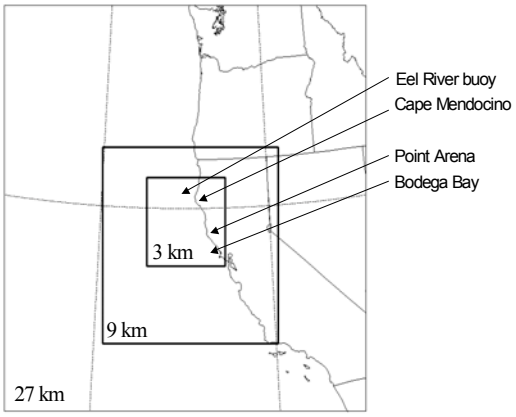

Figure 1. Location of nests.

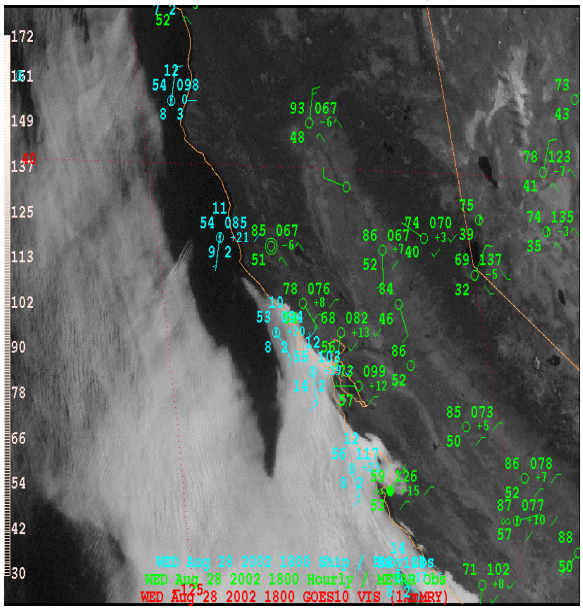

Figure 2. Satellite images from 28 August 2002 valid at a) 1800 UTC and b) 2200 UTC. Surface observations are plotted using the standard station model with wind in kt, temperature and dew point in °F, and pressure in mb.

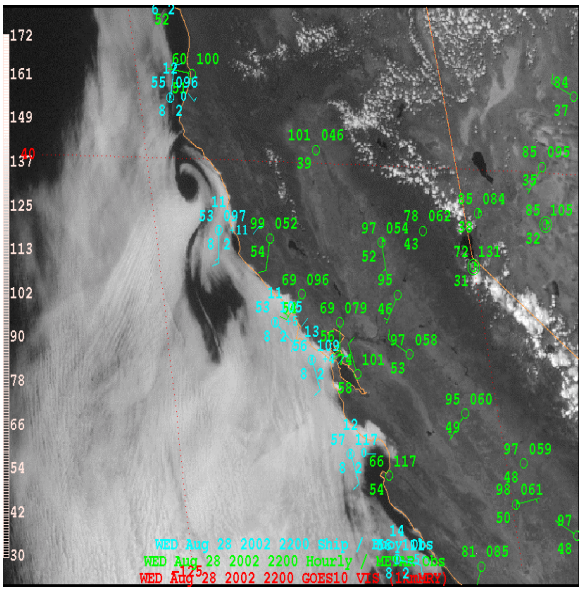

Figure 2 b.

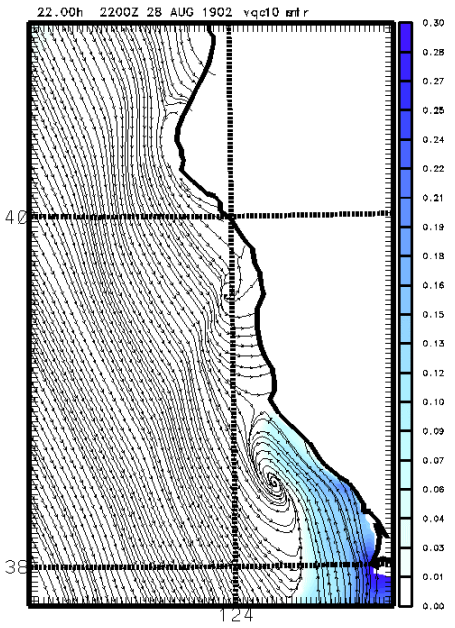

Figure 3. Model forecast streamlines and integrated cloud liquid water (kg m^{-2}; shaded) from a zoomed area of the inner (9 km) nest valid at a) 2200 UTC 28 August 2002; b) 0200 UTC 29 August.

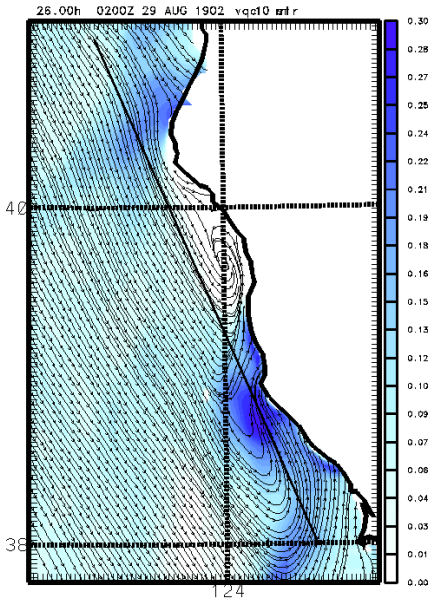

Figure 3b.

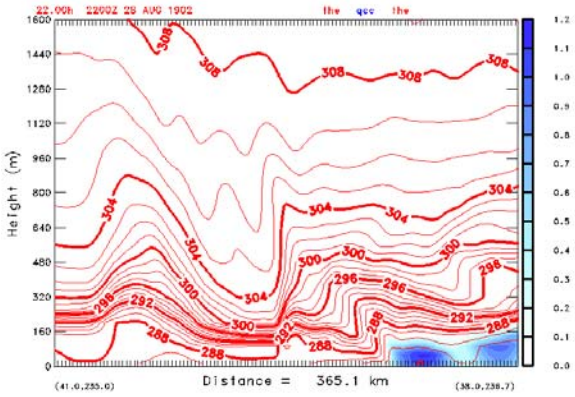

Figure 4. Model forecast cross sections in the plane indicated in Fig 3b extending to 1600 m valid 2200 UTC 28 August showing potential temperature (K) and cloud liquid water mixing ratio (gm/kg).

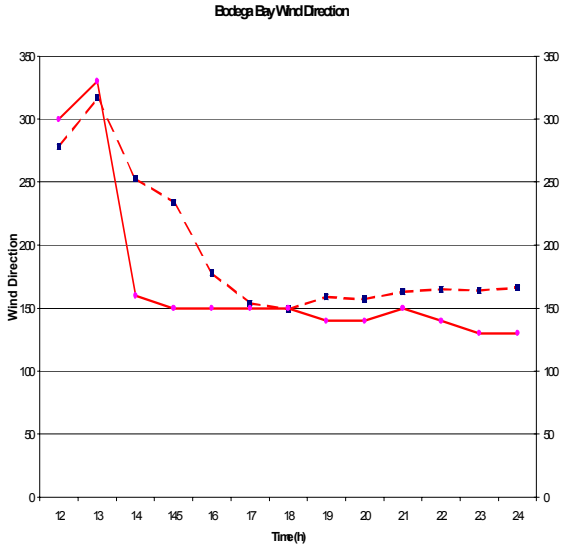

Figure 5. Time series at Bodega Bay from the buoy observation (solid line) and from the mode (dashed line) for wind direction.

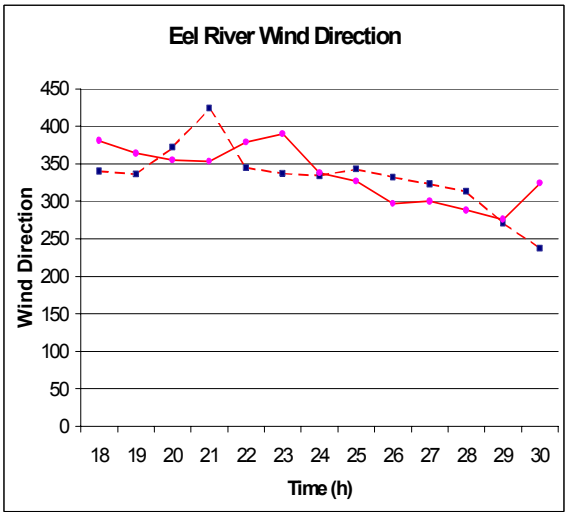

Figure 6. As in Fig. 5 but for Eel River . For wind direction d < 90^{o}, d=d+360 for ease of comparison.